

Neuro-Fuzzy Control with a Novel Training Method Based-on Sliding Mode Control Theory: Application to Tractor Dynamics

Erdal Kayacan, Erkan Kayacan, Herman Ramon,
Wouter Saeys

*Division of Mechatronics, Biostatistics and Sensors (MeBioS),
Department of Biosystems, Katholieke Universiteit Leuven,
Kasteelpark Arenberg 30, B-3001 Leuven, Belgium.
e-mail: {erdal.kayacan, erkan.kayacan, herman.ramon,
wouter.saeys}@biw.kuleuven.be*

Abstract: Accurate automatic guidance of agricultural vehicles is essential for gaining the ultimate benefit in agriculture. As an agricultural vehicle, tractors have more than one subsystem interacting each other, e.g. yaw dynamics, longitudinal dynamics, implement dynamics, etc. Instead of modeling the subsystem interaction prior to model-based control, we have developed a control algorithm which learns the interactions by using the measured feedback error. In this study, two PD controllers and two fuzzy neural networks are combined for controlling the yaw and traction dynamics. While the former ensures the stability of the related subsystem, the latter learns the system dynamics and becomes the leading controller. The interactions between both subsystems are not taken into account explicitly, but are considered to be disturbances in the control of each individual subsystem. A novel sliding mode control theory-based learning algorithm is used to train the fuzzy neural networks, and the convergence of the parameters is shown using a Lyapunov function.

Keywords: Fuzzy neural networks, Sliding mode control, Feedback error learning.

1. INTRODUCTION

As the worldwide food consumption is ever increasing while the arable area is rather limited, increasing agricultural productivity remains an important challenge for mankind. Automation of agricultural machinery is one of the ways to improve the efficiency and productivity of various field operations. In the last decades, dimensions and capacity of the machinery have expanded and the productivity per hectare has increased at a very high rate. The economic pressure, the continuously growing world population and the increasing cost of manpower, force agriculture to produce in a cost and labor efficient way. To increase efficiency and to lighten the job of the people employed in agriculture, there is a need for automation of the tasks performed by the operator. An important task of the machine operator during field operation is steering the machinery accurately across the field. For example, during planting it is very important to plant the new rows perfectly parallel and at equal distance to the previous rows to facilitate mechanical weeding where the weed harrow has to be carefully positioned with respect to the crop rows to avoid damaging the crop. This can be a challenging and very tiring job. Moreover, it has been observed that the

steering accuracy decreases when more actions are asked from the operator or when he gets tired. Therefore, several automatic guidance systems have been developed, some of which are already available on the market.

While RTK-GPS can provide very good absolute positioning accuracy, the performance of the currently available machine guidance systems is rather limited due to the poor performance of the automatic control systems used for this purpose. The main reasons for this poor performance are the complex vehicle kinematics and the large variation in soil conditions which make that the PID controllers used for these machine guidance systems have to be tuned very conservatively. By this conservative tuning robustness of the controller is obtained at the price of performance. Moreover, the constraints of the mechanical system cannot be taken into account directly in these controllers, such that the ad hoc implementation of these constraints can lead to suboptimal behavior of the system.

In this paper, as a solution to the problems of the conventional controllers mentioned above, feedback error learning (FEL) method is proposed as a model-free approach for controlling the tractor dynamics. This method allows us to take the impacts of other subsystems as the disturbances into account. Moreover, the learning part in FEL is able to adapt the parameters of the controllers of the tractor model to soil conditions. Therefore, the potential of FEL strategy for autonomous guidance of a small agricultural tractor is investigated in this study.

* This work has been carried out within the framework of the LeCoPro project (grant nr. 80032) founded by the Institute for the Promotion of Innovation through Science and Technology in Flanders (IWT-Vlaanderen). Wouter Saeys is funded as postdoctoral fellow of the Research Foundation - Flanders (FWO).

2. PROBLEM STATEMENT

In most cases, larger scale mechatronic systems can be divided into different subsystems, where each subsystem has its own characteristics and can be modeled and controlled separately by means of its own inputs and outputs. However, when the subsystem controllers are not aware of the interactions between the different subsystems, they will behave *selfish* and may deteriorate the performance of the other subsystem controllers. Therefore, the combination of optimal subsystem controllers will often not result in optimal control of the global system. By consequence, it is important to make the subsystem controllers aware of the interactions between the different subsystems. When the subsystems are controlled by a model-based controller, the subsystem model should thus combine the states and inputs of the local subsystem and the impact from the other subsystems.

If the impact from other units to the subsystem is known, model-based approaches can be used to model the interactions between the mechatronic subsystems. However, most of the time, the interactions between mechatronics subsystems are not so clear such that they cannot be easily modeled. In such cases, either a polynomial approximation of the real model structure can be used for which the major variables influencing the output of the subsystem of interest are identified through the use of genetic algorithms or the interaction models can be estimated using model-free techniques such as fuzzy logic theory, artificial neural networks and fuzzy neural networks (FNNs).

FEL method was originally proposed in Kawato et al. (1988) for robot control in which a neural network is working with a PD controller. The output of the PD controller is used as a learning error signal to train the neural network. In this paper, this method is applied to FNNs. Instead of trying to minimize an error function, the learning parameters are tuned by the proposed algorithm in a way to enforce the error to satisfy a stable equation. The parameter update rules of FNNs are generated and the learning algorithms for FNN using Lyapunov sense of stability is proven. The learning algorithm proposed in this paper is tested on a large scale mechatronics system which consists of traction dynamics and yaw dynamics of a tractor. In this study, the interactions between the mechatronics subsystems have been modeled as a disturbance to each other.

The main body of the paper contains five sections: In section III, the mathematical model of a tractor is given. In Section IV, the proposed sliding mode feedback-error-learning approach is presented, and the parameter update rules for FNNs are proposed for the case of Gaussian membership functions. In Section V, the simulation results are given. Finally, in Section VI, conclusions are presented.

3. THE MATHEMATICAL MODEL OF A TRACTOR

3.1 Yaw Motion Dynamics

The velocities and the sideslip angles at different locations of the tractor are presented in Fig. 1(a). Similarly, the forces at different locations of the tractor are shown in Fig. 1(b).

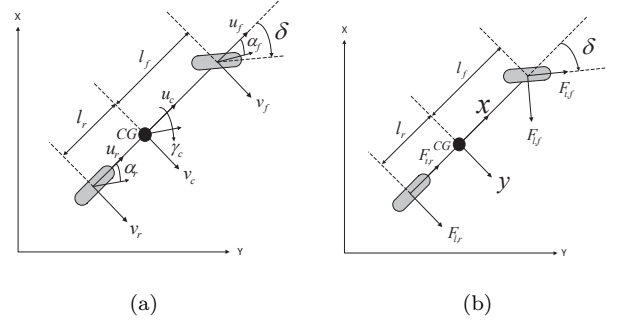


Fig. 1. Dynamic bicycle model for a tractor: (a) velocities and slip angles (b) forces at different locations of the system

The lateral dynamics of the tractor can be written as follows Karkee and Steward (2010):

$$m(\dot{v}_c + u_c \gamma) = F_{t,f} \sin \delta + F_{l,f} \cos \delta + F_{l,r} \quad (1)$$

where m , $F_{t,f}$, $F_{l,f}$, $F_{l,r}$ represent the mass of the tractor, the traction and lateral forces on the front wheel, the lateral force on the rear wheel, respectively.

The yaw dynamics of the tractor are written as follows:

$$I_z \dot{\gamma} = l_f (F_{t,f} \sin \delta + F_{l,f} \cos \delta) - l_r F_{l,r} \quad (2)$$

where l_f , l_r and I_z respectively represent the distance between the front axle and the center of gravity of the tractor, the distance between the rear axle and the center of gravity of the tractor, and the moment of inertia of the tractor.

The tire side slip angles must be calculated in order to determine the forces caused by the slip. It is assumed that the steering angle of the front wheel is small, and this allows to the following approximations: $\sin \delta \approx \delta$ and $\cos \delta \approx 1$. The side slip angles of the front and the rear tires are written as follows:

$$\alpha_f = \frac{v_c + l_f \gamma}{u_c} - \delta \quad \text{and} \quad \alpha_r = \frac{v_c - l_r \gamma}{u_c} \quad (3)$$

To determine the lateral force on the tire, there are many different approaches in literature. In this study, the lateral tire forces are calculated using a linear model which assumes these to be proportional to the slip angles in Piyabongkarn et al. (2009); Geng et al. (2009)

$$F_{l,i} = -C_{\alpha,i} \alpha_i \quad i = \{f, r\} \quad (4)$$

where $C_{\alpha,i}$, $i = \{f, r\}$, represents the cornering stiffness of the tires of the tractor. The tire cornering stiffness parameters are the averaged slopes of the lateral force characteristics in this method.

The equations of motion of the tractor are written in state space form by combining (1), (2), (3) and (4) as follows:

$$\begin{bmatrix} \dot{v}_c \\ \dot{\gamma} \end{bmatrix} = \begin{bmatrix} A_{11} & A_{12} \\ A_{21} & A_{22} \end{bmatrix} \begin{bmatrix} v_c \\ \gamma \end{bmatrix} + \begin{bmatrix} b_1 \\ b_2 \end{bmatrix} \delta \quad (5)$$

where

$$\begin{aligned}
A_{11} &= -\frac{C_{\alpha,f} + C_{\alpha,r}}{mu_c}, \\
A_{12} &= \frac{-l_f C_{\alpha,f} + l_r C_{\alpha,r}}{mu_c} - u_c, \\
A_{21} &= \frac{-l_f C_{\alpha,f} + l_r C_{\alpha,r}}{I_z u_c}, \\
A_{22} &= -\frac{l_f^2 C_{\alpha,f} + l_r^2 C_{\alpha,r}}{I_z u_c}, \\
b_1 &= \frac{C_{\alpha,f}}{m} \quad \text{and} \quad b_2 = \frac{l_f C_{\alpha,f}}{I_z}
\end{aligned} \tag{6}$$

3.2 Traction Dynamics

A quarter vehicle dynamics model is used to describe the traction dynamics of the vehicle. In this approach, the system model is written as follows:

$$\begin{aligned}
I\dot{\omega} &= -rF_t + T \\
m\dot{u}_c &= F_t
\end{aligned} \tag{7}$$

where I, ω, u_c, r, F_t and T represent respectively the inertial moment of the wheels of the vehicle, the angular velocity of the wheels of the vehicle, the linear velocity of the wheel of the vehicle, the radius of the wheels of the vehicle, the traction force and the torque on the wheel of the vehicle. These parameters are schematically illustrated in Fig. 2.

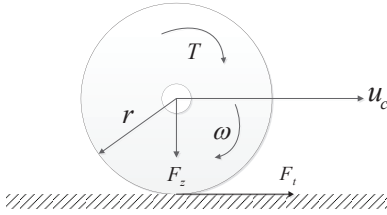


Fig. 2. The schematic view of the wheel

In order to reflect the effect from the yaw dynamics on the longitudinal dynamics in real-life, an extra term has been added to the model which is function of yaw rate. This term always tries to decrease longitudinal velocity. It has also a coefficient K , which can be chosen arbitrarily. The interconnection term that describes the influence of the yaw dynamics of the tractor is added into (7) as follows:

$$\begin{aligned}
I\dot{\omega} &= -rF_t + T - Kr |\gamma| \\
m\dot{u}_c &= F_t - K |\gamma|
\end{aligned} \tag{8}$$

where K represents the coefficient of the interaction term.

The traction force is written as follows:

$$\mu(s_j, c) = \frac{F_{t,j}}{F_{z,j}} \quad j = \{f, r\} \tag{9}$$

where $\mu(s_j, c), F_{t,j}$ and $F_{z,j}$ represent the adhesion coefficient, the traction force on the tire and the nominal vertical force at wheel contact, respectively.

The longitudinal slip ratio is defined as follows:

$$s = \begin{cases} \frac{r\omega}{u_c} - 1 & \text{if } u_c > r\omega, u_c \neq 0 \text{ for braking} \\ 1 - \frac{u_c}{r\omega} & \text{if } u_c < r\omega, r\omega \neq 0 \text{ for driving} \end{cases}$$

where s, r and ω represent the longitudinal slip ratio, the radius of the wheel and the angular velocity of the wheel, respectively. The adhesion coefficient is written as follows:

$$\mu(s) = \frac{2\mu_p s_p s}{s_p^2 + s^2} \tag{10}$$

where μ_p and s_p are the peak values for various road conditions.

4. THE ADAPTIVE FUZZY NEURAL CONTROL APPROACH

4.1 The Control Scheme and the Fuzzy Neuro Network Structure

Figure 3 shows the proposed control scheme used in this study. The PD controllers are provided both as an ordinary feedback controller to guarantee global asymptotic stability in compact space and as an inverse reference model of the response of the system under control.

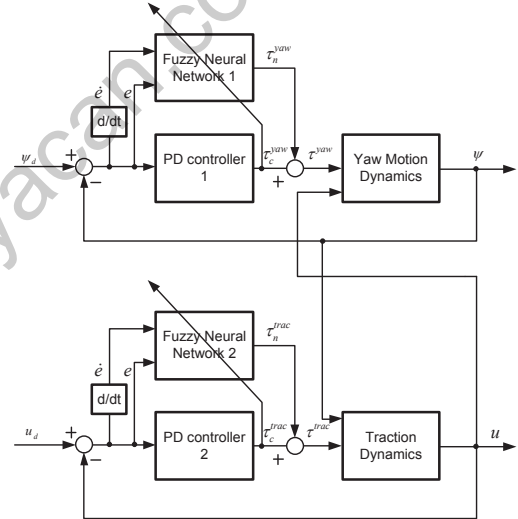


Fig. 3. Block diagram of the proposed adaptive fuzzy neuro control scheme

4.2 Fuzzy Neural Network (FNN)

The incoming signals, $x_1(t)=e(t)$ and $x_2(t)=\dot{e}(t)$, are fuzzified by using Gaussian membership functions, which are defined by their corresponding membership functions $\mu_{1_i}(x_1)$ and $\mu_{2_j}(x_2)$ for $i = 1, \dots, I$ and $j = 1, \dots, J$.

The fuzzy *if-then* rule R_{ij} of a zeroth-order TSK model with two input variables can be defined as follows:

$$R_{ij}: \text{If } x_1 \text{ is } M_{1_i} \text{ and } x_2 \text{ is } M_{2_j}, \text{ then } f_{ij}=d_{ij}$$

where d_{ij} is a given constant.

The strength of the rule R_{ij} is obtained as a T -norm of the membership functions in the premise part (by using a multiplication operator):

$$W_{ij} = \mu_{1_i}(x_1)\mu_{2_j}(x_2) \tag{11}$$

The Gaussian membership functions $\mu_{1_i}(x_1)$ and $\mu_{2_j}(x_2)$ of the inputs x_1 and x_2 in the above expression have the following appearance:

$$\mu_{1_i}(x_1) = \exp \left[-\frac{(x_1 - c_{1_i})^2}{\sigma_{1_i}^2} \right] \quad (12)$$

$$\mu_{2_j}(x_2) = \exp \left[-\frac{(x_2 - c_{2_j})^2}{\sigma_{2_j}^2} \right] \quad (13)$$

where the real constants $c, \sigma > 0$ are among the tunable parameters of the above fuzzy neural structure.

By inserting (12) and (13) into (11), the following expression is obtained:

$$W_{ij} = \exp \left[-\frac{(x_1 - c_{1_i})^2}{\sigma_{1_i}^2} - \frac{(x_2 - c_{2_j})^2}{\sigma_{2_j}^2} \right] \quad (14)$$

The output signal of the FNN $\tau_n(t)$ is calculated as a weighted average of the output of each rule Jin (2003):

$$\tau_n(t) = \frac{\sum_{i=1}^I \sum_{j=1}^J f_{ij} W_{ij}}{\sum_{i=1}^I \sum_{j=1}^J W_{ij}} \quad (15)$$

After normalization of (15), the output signal of the FNN will acquire the following form:

$$\tau_n(t) = \sum_{i=1}^I \sum_{j=1}^J f_{ij} \bar{W}_{ij} \quad (16)$$

where \bar{W}_{ij} is the normalized value of the output signal of the neuron ij from the second hidden layer of the network:

$$\bar{W}_{ij} = \frac{W_{ij}}{\sum_{i=1}^I \sum_{j=1}^J W_{ij}} \quad (17)$$

The input signal τ to the system to be controlled is as follows:

$$\tau = \tau_c - \tau_n \quad (18)$$

where τ_c and τ_n are the control signals generated by the PD controller and the FNN, respectively.

Due to the control scheme adopted (Fig. 3), where the conventional controllers serve to guarantee global asymptotic stability in compact space, the input signals $x_1(t)$ and $x_2(t)$, and their time derivatives can be considered bounded:

$$|x_1(t)| \leq B_x, \quad |x_2(t)| \leq B_x \quad \forall t \quad (19)$$

$$|\dot{x}_1(t)| \leq B_{\dot{x}}, \quad |\dot{x}_2(t)| \leq B_{\dot{x}} \quad \forall t \quad (20)$$

where B_x and $B_{\dot{x}}$ are assumed to be some known positive constants.

From (11)-(17) and (19)-(20), it follows that $0 < \bar{W}_{ij} \leq 1$. In addition it can be easily seen from (17) that $\sum_{i=1}^I \sum_{j=1}^J \bar{W}_{ij} = 1$.

Similarly, τ and $\dot{\tau}$ are bounded signals too, *i.e.*

$$|\tau(t)| \leq B_\tau, \quad |\dot{\tau}(t)| \leq B_{\dot{\tau}} \quad \forall t \quad (21)$$

where B_τ and $B_{\dot{\tau}}$ are some known positive constants.

4.3 The Sliding Mode Learning Algorithm

Using sliding mode control (SMC) theory principles, the zero value of the learning error coordinate $\tau_c(t)$ can be defined as a time-varying sliding surface:

$$S_c(\tau_n, \tau) = \tau_c(t) = \tau_n(t) + \tau(t) = 0 \quad (22)$$

The sliding surface for the nonlinear system under control $S_p(e, \dot{e})$ is defined as:

$$S_p(e, \dot{e}) = \dot{e} + \chi e \quad (23)$$

with χ being a constant determining the slope of the sliding surface.

A sliding motion will appear on the sliding manifold $S_c(\tau_n, \tau) = \tau_c(t) = 0$ after a time t_h , if the condition $S_c(t)\dot{S}_c(t) = \tau_c(t)\dot{\tau}_c(t) < 0$ is satisfied for all t in some nontrivial semi-open subinterval of time of the form $[t, t_h) \subset (0, t_h)$.

It is desired to devise a dynamical feedback adaptation mechanism, or online learning algorithm for the FNN parameters such that the sliding mode condition of the above definition is enforced.

The Parameter Update Rules for the FNN

Theorem 1. If the adaptation laws for the parameters of the considered FNN are chosen respectively as:

$$\dot{c}_{1_i} = \dot{x}_1 \quad (24)$$

$$\dot{c}_{2_j} = \dot{x}_2 \quad (25)$$

$$\dot{\sigma}_{1_i} = -\frac{(\sigma_{1_i})^3}{(x_1 - c_{1_i})^2} \alpha \text{sgn}(\tau_c) \quad (26)$$

$$\dot{\sigma}_{2_j} = -\frac{(\sigma_{2_j})^3}{(x_2 - c_{2_j})^2} \alpha \text{sgn}(\tau_c) \quad (27)$$

$$\dot{f}_{ij} = -\frac{\bar{W}_{ij}}{\bar{W}^T \bar{W}} \alpha \text{sign}(\tau_c) \quad (28)$$

where α is a sufficiently large positive design constant satisfying the following inequality:

$$\alpha > B_{\dot{\tau}} \quad (29)$$

then, given an arbitrary initial condition $\tau_c(0)$, the learning error $\tau_c(t)$ will converge to zero during a finite time t_h .

The following vector in (28) has been specified as follows:

$$\bar{W}(t) = [\bar{W}_{11}(t) \ \bar{W}_{12}(t) \ \dots \ \bar{W}_{ij}(t) \ \dots \ \bar{W}_{IJ}(t)]^T$$

Proof. The reader is referred to Appendix A.

The relation between the sliding line S_p and the zero adaptive learning error level S_c , if χ is taken as $\chi = \frac{k_p}{k_D}$, is determined by the following equation:

$$S_c = \tau_c = k_D \dot{e} + k_p e = k_D \left(\dot{e} + \frac{k_p}{k_D} e \right) = k_D S_p \quad (30)$$

The tracking performance of the feedback control system can be analyzed by introducing the following Lyapunov function candidate:

$$V_p = \frac{1}{2} S_p^2 \quad (31)$$

Theorem 2. If the adaptation strategy for the adjustable parameters of the FNN is chosen as in (24)-(28), then the negative definiteness of the time derivative of the Lyapunov function in (31) is ensured.

Proof. The reader is referred to Appendix B.

Remark: The obtained result means that, assuming the SMC task is achievable, using τ_c as a learning error for the FNN together with the adaptation laws (24)-(28) enforces the desired reaching mode followed by a sliding regime for the system under control.

5. SIMULATION STUDIES

The numerical values used in this study are $m = 9391 \text{ kg}$, $I_z = 35709 \text{ kg m}^2$, $l_f = 1.7 \text{ m}$, $l_r = 1.2 \text{ m}$, $C_{\alpha,f} = 220 \text{ KN rad}^{-1}$ and $C_{\alpha,r} = 486 \text{ KN rad}^{-1}$. These numerical values are collected from a John Deere MFWD tractor (model 7930, Deere and Co., Moline IL) Karkee and Steward (2010). The sampling period of the simulations is set to 0.1 s . The number of membership functions for input 1 and input 2 is set to $I = J = 3$ for all the simulations.

While the coefficients of the PD controller for the yaw motion dynamics are set to $k_p = 0.1$ and $k_d = 0.001$, the coefficients for the traction dynamics are set to $k_p = 70000$ and $k_d = 20$ by trial-and-error method. The learning rates for the FNN 1 and FNN 2 are set to $1 \alpha_1 = 10^{-2}$ and $2 \alpha_2 = 25$, respectively. The coefficient of the interaction model in (8) is set to $K = 50000$. During the simulations, all the weight matrices in both premise and consequent part of the rules are initialized randomly. The adhesion coefficient μ is set to 0.6 . The maximum interaction between the wheels and the surface occurs when the peak value of the longitudinal slip is $s_p = 0.2$.

The following reference signals are applied to the system:

$$\text{Reference}(t) = \begin{cases} \psi_{ref}(t) = 0.6\sin(0.005t)\text{rad} \\ u_{cref}(t) = 5\text{m/s} \end{cases} \quad (32)$$

As can be seen from Fig. 5, when the PD controllers act alone, the control performances of both the longitudinal dynamics and yaw dynamics are not reasonable. The steady state errors both in yaw and longitudinal dynamics are non-zero. The fine tuning of such controllers in real life is challenging, because in addition to the interactions of the subsystems, there exist unmodeled dynamics and uncertainties in real world applications.

Figure 5 shows the condition when the PD controllers are working in parallel with the FNNs in which the control performance of both longitudinal dynamics and yaw dynamics are improved. These results indicate that FNNs are able to learn the system dynamics after a while, and they can improve the overall performance of the system without the need of fine tuning the conventional controllers which is a very demanding process in real-life applications.

Figure 6 shows the control signals coming from the conventional PD controllers and FNNs. As can be seen from Fig. 6, at the beginning, the dominating control signals are the ones coming from the PD controllers. After a short time, using the control signal τ_c , the FNNs are able to take over the control, thus becoming the leading controllers. This shows that PD controllers ensure the stability of the system while the FNNs learn the system dynamics and take the responsibility of the controlling of the vehicle in the proposed control algorithm.

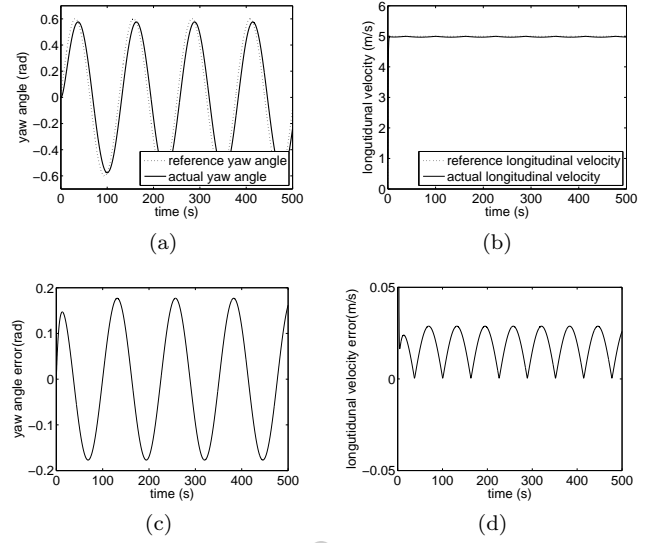


Fig. 4. PD controllers working alone: (a) Yaw angle response (b) Longitudinal velocity response (c) Yaw angle error (d) Longitudinal velocity error

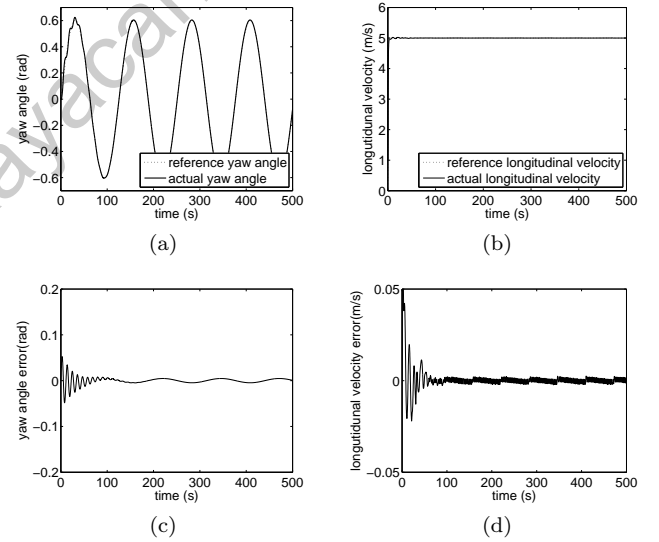


Fig. 5. PD controllers working in parallel with FNNs: (a) Yaw angle response (b) Longitudinal velocity response (c) Yaw angle error (d) Longitudinal velocity error

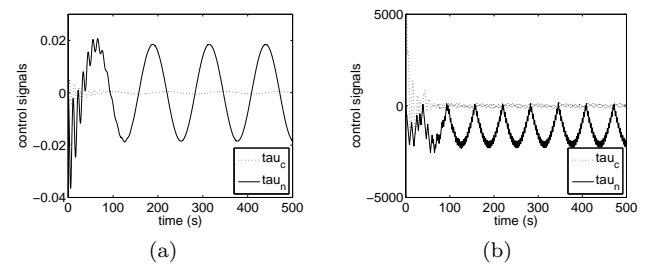


Fig. 6. (a) The control signals coming from PD controller 1 and FNN 1 (b) The control signals coming from PD controller 2 and FNN 2

6. CONCLUSION

The proposed control scheme consisting of two conventional PD controllers working in parallel with two FNNs is tested on a tractor model which has two subsystems interacting with each other. For each subsystem, the control structure proposed consists of a PD controller and a FNN which is capable of learning the plant model online instead of using accurate predefined dynamical equations of the system. The use of the combination of fuzzy logic control, artificial neural networks and sliding mode control theory harmoniously allows us to better handle the interactions in the subsystems, uncertainties and lack of modeling information. In addition to its robustness, another prominent feature is the computational simplicity of the proposed approach. Encouraged by these simulation results, an experimental investigation is about to be launched.

REFERENCES

- Geng, C., Mostefai, L., Dena, M., and Hori, Y. (2009). Direct yaw-moment control of an in-wheel-motored electric vehicle based on body slip angle fuzzy observer. *IEEE Transactions on Industrial Electronics*, 56(5), 1411 – 1419.
- Jin, Y. (2003). *Advanced Fuzzy Systems Design and Applications*. Physica-Verlag.
- Karkee, M. and Steward, B.L. (2010). Study of the open and closed loop characteristics of a tractor and a single axle towed implement system. *Journal of Terramechanics*, 47(6), 379 – 393.
- Kawato, M., Uno, Y., Isobe, M., and Suzuki, R. (1988). Hierarchical neural network model for voluntary movement with application to robotics. *Control Systems Magazine, IEEE*, 8(2), 8 – 15.
- Piyabongkarn, D., Rajamani, R., Grogg, J.A., and Lew, J.Y. (2009). Development and experimental evaluation of a slip angle estimator for vehicle stability control. *IEEE Transactions on Control Systems Technology*, 17(1), 78 – 88.

Appendix A. PROOF OF THEOREM 1

The time derivatives of (12) and (13) are as follows:

$$\dot{\mu}_{1i}(x_1) = -2A_{1i}(A_{1i})'\mu_{1i}(x_1) \quad (\text{A.1})$$

$$\dot{\mu}_{2j}(x_2) = -2A_{2j}(A_{2j})'\mu_{2j}(x_2) \quad (\text{A.2})$$

where

$$A_{1i} = \left(\frac{x_1 - c_{1i}}{\sigma_{1i}} \right) \quad \text{and} \quad A_{2j} = \left(\frac{x_2 - c_{2j}}{\sigma_{2j}} \right) \quad (\text{A.3})$$

The time derivative of (17) can be obtained as follows:

$$\dot{\bar{W}}_{ij} = -\bar{W}_{ij}\dot{K}_{ij} + \bar{W}_{ij} \sum_{i=1}^I \sum_{j=1}^J (\bar{W}_{ij}\dot{K}_{ij}) \quad (\text{A.4})$$

where

$$\dot{K}_{ij} = 2 \left(A_{1i}(A_{1i})' + A_{2j}(A_{2j})' \right)$$

By using the following Lyapunov function, the stability condition can be checked:

$$V_c = \frac{1}{2}\tau_c^2(t) \quad (\text{A.5})$$

The time derivative of V_c is given by:

$$\dot{V}_c = \tau_c \dot{\tau}_c = \tau_c(\dot{\tau}_n + \dot{\tau}) \quad (\text{A.6})$$

where

$$\dot{\tau}_n = \sum_{i=1}^I \sum_{j=1}^J (\dot{f}_{ij}\bar{W}_{ij} + f_{ij}\dot{\bar{W}}_{ij}) \quad (\text{A.7})$$

By replacing (A.7) to the (A.6), (A.8) is obtained:

$$\begin{aligned} \dot{V}_c &= \tau_c \left(\sum_{i=1}^I \sum_{j=1}^J \left(\dot{f}_{ij}\bar{W}_{ij} + f_{ij} \left(-\bar{W}_{ij}\dot{K}_{ij} \right. \right. \right. \\ &\quad \left. \left. \left. + \bar{W}_{ij} \sum_{i=1}^I \sum_{j=1}^J \bar{W}_{ij}\dot{K}_{ij} \right) \right) + \dot{\tau} \right) \\ &= \tau_c \left[\sum_{i=1}^I \sum_{j=1}^J \dot{f}_{ij}\bar{W}_{ij} - 2 \sum_{i=1}^I \sum_{j=1}^J \bar{W}_{ij} \left(A_{1i}(A_{1i})' \right. \right. \\ &\quad \left. \left. + A_{2j}(A_{2j})' \right) f_{ij} \right. \\ &\quad \left. + 2 \sum_{i=1}^I \sum_{j=1}^J \left(\bar{W}_{ij} f_{ij} \sum_{i=1}^I \sum_{j=1}^J \bar{W}_{ij} \left(A_{1i}(A_{1i})' \right. \right. \right. \\ &\quad \left. \left. \left. + A_{2j}(A_{2j})' \right) \right) + \dot{\tau} \right] \end{aligned} \quad (\text{A.8})$$

where

$$\dot{A}_{1i} = \frac{(x_1 - c_{1i})\sigma_{1i} - (x_1 - c_{1i})\dot{\sigma}_{1i}}{\sigma_{1i}^2}$$

$$\dot{A}_{2j} = \frac{(x_2 - c_{2j})\sigma_{2j} - (x_2 - c_{2j})\dot{\sigma}_{2j}}{\sigma_{2j}^2}$$

Equation (A.9) can be obtained by using (24)-(27);

$$A_{1i}\dot{A}_{1i} = A_{2j}\dot{A}_{2j} = \alpha \text{sgn}(\tau_c) \quad (\text{A.9})$$

$$\begin{aligned} \dot{V}_c &= \tau_c \left[\sum_{i=1}^I \sum_{j=1}^J \dot{f}_{ij}\bar{W}_{ij} - 4 \sum_{i=1}^I \sum_{j=1}^J \bar{W}_{ij} (\alpha \text{sgn}(\tau_c)) f_{ij} + \right. \\ &\quad \left. + 4 \sum_{i=1}^I \sum_{j=1}^J \left(\bar{W}_{ij} f_{ij} \sum_{i=1}^I \sum_{j=1}^J \bar{W}_{ij} (\alpha \text{sgn}(\tau_c)) \right) + \dot{\tau} \right] \\ &= \tau_c \left[\sum_{i=1}^I \sum_{j=1}^J \dot{f}_{ij}\bar{W}_{ij} + \dot{\tau} \right] \end{aligned}$$

where

$$\dot{f}_{ij} = -\frac{\bar{W}_{ij}}{\bar{W}^T \bar{W}} \alpha \text{sign}(\tau_c) \quad (\text{A.10})$$

$$\begin{aligned} \dot{V}_c &= \tau_c \left[-\alpha \text{sgn}(\tau_c) + \dot{\tau} \right] \\ &= \left[-\alpha |\tau_c| + |\tau_c| B_{\dot{\tau}} \right] < 0 \quad (\text{A.11}) \end{aligned}$$

Appendix B. PROOF OF THEOREM 2

Evaluating the time derivative of the Lyapunov function in (31) yields:

$$\begin{aligned} \dot{V}_p &= \dot{S}_p S_p = \frac{1}{k_D^2} \dot{S}_c S_c \\ &\leq \frac{|\tau_c|}{k_D^2} \left[-\alpha + B_{\dot{\tau}} \right] < 0, \quad \forall S_c, S_p \neq 0 \end{aligned} \quad (\text{B.1})$$